

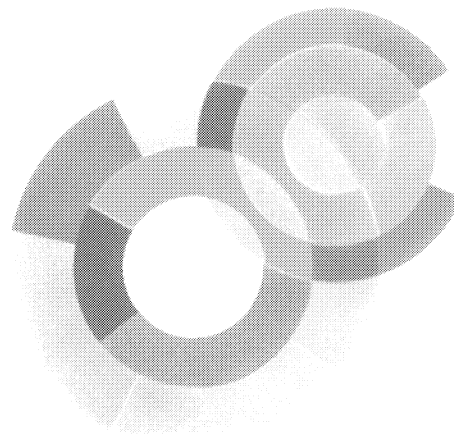


# DAPNIA

CERN LIBRARIES, GENEVA



CM-P00061930



DAPNIA-06-146

06/2006

**Recent developments  
in electromagnetic hadron form factors**

E. Tomasi-Gustafsson, E. A. Kuraev, Yu. M. Bystritskiy

*11<sup>th</sup> International Conference on Nuclear Reaction Mechanisms,  
Varenna (Italy), June 12-16, 2006*

Département d'Astrophysique, de Physique des Particules, de Physique Nucléaire et de l'Instrumentation Associée

DSM/DAPNIA, CEA/Saclay F - 91191 Gif-sur-Yvette Cédex

Tél : (1) 69 08 24 02 Fax : (1) 69 08 99 89

[http : //www-dapnia.cea.fr](http://www-dapnia.cea.fr)

# RECENT DEVELOPMENTS IN ELECTROMAGNETIC HADRON FORM FACTORS

E. Tomasi-Gustafsson\*

*DAPNIA/SPhN, CEA/Saclay  
91191 Gif-sur-Yvette Cedex, France*

E. A. Kuraev and Yu. M. Bystritskiy

*JINR-BLTP, 141980 Dubna  
Moscow region, Russian Federation*

June 26, 2006

New data on electromagnetic hadron form factors have triggered large theoretical and experimental efforts and inspired new ideas and several proposals at different accelerators. The possibility to achieve  $Q^2$  values up to  $\simeq 6 \text{ GeV}^2$  and the inconsistencies among form factors extracted from polarized and unpolarized experiments suggest to search for the two-photon contribution. A calculation of radiative corrections based on the structure function method can bring the results into agreement and shows that the two photon contribution to electron proton elastic scattering is small.

## 1 Introduction

The experimental determination of the elastic proton electromagnetic form factors (FFs) at large momentum transfer is presently of large interest, due to the availability of electron beams in the GeV range with high intensity and high polarization, large acceptance spectrometers, hadron polarized targets, and hadron polarimeters. The possibility of extending the measurements of such fundamental quantities, which contain dynamical information on the nucleon structure, has inspired experimental programs at JLab, Frascati and at future machines, such as GSI, both in the space-like and in the time-like regions.

The traditional way to measure proton electromagnetic FFs consists in the determination of the  $\epsilon$  dependence of the reduced elastic differential cross section, which may be written, assuming that the interaction occurs through the exchange of one-photon, as [1]:

$$\sigma_{red}^{Born}(\theta, Q^2) = \epsilon(1 + \tau) \left[ 1 + 2\frac{E}{m} \sin^2(\theta/2) \right] \frac{4E^2 \sin^4(\theta/2)}{\alpha^2 \cos^2(\theta/2)} \frac{d\sigma}{d\Omega} = \tau G_M^2(Q^2) + \epsilon G_E^2(Q^2), \quad (1)$$

where  $\epsilon = [1 + 2(1 + \tau) \tan^2(\theta/2)]^{-1}$ ,  $\alpha = 1/137$ ,  $\tau = Q^2/(4m^2)$ ,  $Q^2$  is the momentum transfer squared,  $m$  is the proton mass,  $E$  and  $\theta$  are the incident electron energy and the scattering angle of the outgoing electron, respectively, and  $G_M(Q^2)$  and  $G_E(Q^2)$  are the magnetic and the electric proton FFs and are functions of  $Q^2$ , only. Measurements of the elastic differential cross section at different angles for a fixed value of  $Q^2$  allow  $G_E(Q^2)$  and  $G_M(Q^2)$  to be determined as the slope and the intercept, respectively, from the linear  $\epsilon$  dependence (1).

---

\*e-mail : etomasi@cea.fr

High precision data on the ratio of the electric to magnetic proton FFs at large  $Q^2$  have been recently obtained [2] through the polarization transfer method [3]. Such data revealed a surprising trend, which deviates from the expected scaling behavior previously obtained through the measurement of the elastic  $ep$  cross section according the Rosenbluth separation method [4]. New precise measurements of the unpolarized elastic  $ep$  cross section [5] and re-analysis of the old data [6, 7] confirm that the behavior of the measured ratio  $R(Q^2) = \mu G_E(Q^2)/G_M(Q^2)$  ( $\mu = 2.79$  is the magnetic moment of the proton) is different depending on the method used: either  $R(Q^2) \simeq 1$ , i.e., scaling behavior for unpolarized cross section measurements, or a strong monotonic decrease from polarization transfer measurements, which has been parametrized as [2]:

$$R(Q^2) = 1 - (0.130 \pm 0.005)\{Q^2 [\text{GeV}^2] - (0.04 \pm 0.09)\}. \quad (2)$$

This puzzle has given rise to many speculations and different interpretations [9], suggesting further experiments. In particular, it has been suggested that the presence of  $2\gamma$  exchange could solve this discrepancy through its interference with the main mechanism ( $1\gamma$  exchange). However, the present data do not give any evidence of the presence of the  $2\gamma$  mechanism, in the limit of the experimental errors [10]. The main reason is that, if one takes into account  $C$ -invariance and crossing symmetry, the  $2\gamma$  mechanism introduces a very specific non linear  $\epsilon$  dependence of the reduced cross section [11], whereas the data do not show any deviation from linearity.

No experimental bias has been found in the measurements: the observables are in one case the unpolarized differential cross section, and in the other case, the polarization of the outgoing proton in the scattering plane (more precisely the ratio between the longitudinal and the transverse polarization).

Let us stress that the discrepancy is not at the level of these observables: it has been shown that constraining the ratio  $R$  from polarization measurements and extracting  $G_M(Q^2)$  from the measured cross section "*the magnetic FF is systematically 1.5-3% larger than had been extracted in previous analysis*", but well inside the error bars [12].

The inconsistency arises at the level of the slope of the  $\epsilon$  dependence of the reduced cross section, which is directly related to  $G_E(Q^2)$ , i.e. the derivative of the differential cross section, with respect to  $\epsilon$ .

Radiative corrections (RC), which depend on the relevant kinematic variables,  $\epsilon$  and  $Q^2$  are applied to the unpolarized cross section and may reach 30-40% at large  $Q^2$ , whereas they are neglected in polarization measurements. The standard procedure is based on Ref. [13], where RC are calculated as a global factor which is applied to the elastic cross section extracted from the data.

However, several approximations are made, which may not be safely extrapolated to the conditions of the present experiments. In particular in the calculation of Ref. [13], the consideration of hard collinear photon emission (where the radiative photon is emitted along the direction of the incident or outgoing electron) is not complete. Moreover higher order RC, pair production as well as vacuum polarization are not included.

We have shown [14] that a large correlation exists between the two parameters extracted from the Rosenbluth fit at large  $Q^2$ . A probable source of these correlations is found in the standard procedure taken for RC. We recalculate the cross section of elastic electron-proton scattering in leading and next-to leading approximation using the electron QED structure (radiation) function approach [15, 16]. Numerical results show that this approach can bring the polarized and unpolarized data into agreement, in frame of one photon exchange.

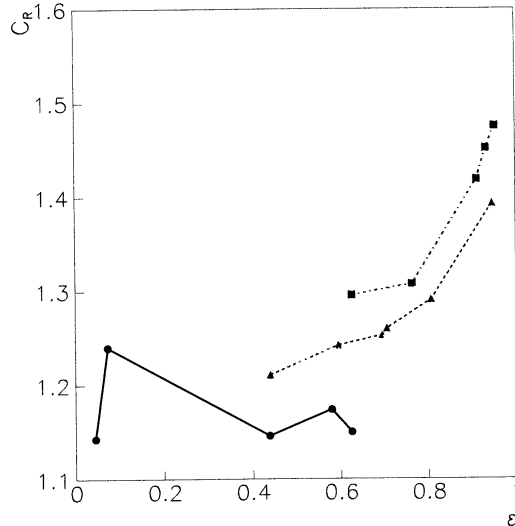


Figure 1: Radiative correction factor applied to the data at  $Q^2=3$  GeV<sup>2</sup> (squares) from Ref. [17], at  $Q^2=4$  GeV<sup>2</sup> (triangles) and 5 GeV<sup>2</sup> (inverted triangles) from Ref. [4], and at  $Q^2=0.32$  GeV<sup>2</sup> from Ref. [18] (circles). The lines are drawn to guide the eye.

## 2 Statistical analysis of the present data

It is known that at large  $Q^2$  the contribution of the electric term to the cross section becomes very small, as the magnetic part is amplified by the kinematic factor  $\tau$ . Assuming the linear dependence of Eq. (2), one can see that, for example, for  $\epsilon = 0.2$  the electric contribution becomes lower than 3% starting from 2 GeV<sup>2</sup>. This number should be compared with the absolute uncertainty of the cross section measurement. When this contribution is larger or is of the same order, the sensitivity of the measurement to the electric term is lost and the extraction of  $G_E(Q^2)$  becomes meaningless.

A large correlation appears in the FFs data extracted with the Rosenbluth method at large  $Q^2$ , that we attribute to the procedure used in applying radiative corrections.

The measured elastic cross section is corrected by a global factor  $C_R$ , according to the prescription [13]:

$$\sigma_{red}^{Born} = C_R \sigma_{red}^{meas}. \quad (3)$$

The factor  $C_R$  contains a large  $\epsilon$  dependence and a smooth  $Q^2$  dependence, and it is common to the electric and magnetic parts. At the largest  $Q^2$  considered here this factor can reach 30-40%, getting larger when the resolution is higher. If one made a linear approximation for the uncorrected data, one might even find a negative slope starting from  $Q^2 \geq 3$  GeV<sup>2</sup> [10].

In Fig. 1 we show the  $C_R$  dependence on  $\epsilon$  for different  $Q^2$  and from different sets of data. One can see that  $C_R$  increases with  $\epsilon$ , rising very fast as  $\epsilon \rightarrow 1$ . It may be different in different experiments because its calculation requires an integration over the experimental acceptance.

The Rosenbluth separation consists of a linear fit to the reduced cross section at fixed  $Q^2$ , where the two parameters are  $G_E^2$  and  $G_M^2$ . The multiplication by a factor which is common to the electric and magnetic terms, see Eqs. (1,3), and depends strongly on  $\epsilon$ , induces a correlation between these two parameters. In order to determine quantitatively how large this correlation is, we have built the error matrix for the Rosenbluth fits to the different sets of data available in the literature.

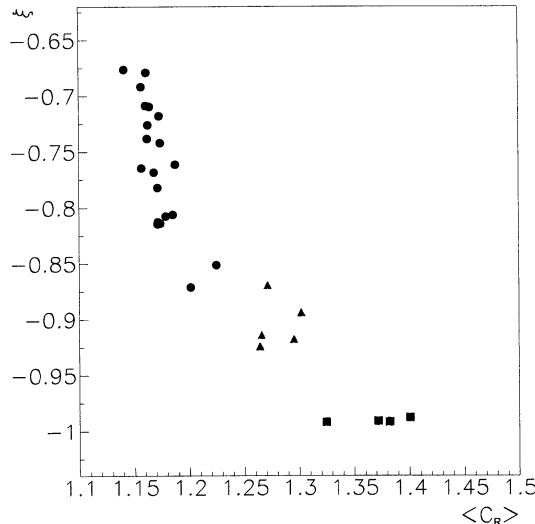


Figure 2: Correlation coefficient,  $\xi$ , as a function of the radiative correction factor  $\langle C_R \rangle$ , averaged over  $\epsilon$ , for different sets of data: from Ref. [18] (circles), from Ref. [4] (triangles) and from Ref. [17] (squares).

At fixed  $Q^2$  the reduced cross section, normalized to the dipole function:  $G_D^2 = [1 + Q^2(\text{GeV}^2)/0.71]^{-2}$ , has been parametrized by a linear  $\epsilon$  dependence:  $\sigma_{red}^{Born}/G_D^2 = a\epsilon + b$ . The two parameters,  $a$  and  $b$ , have been determined for each set of data as well as their errors  $\sigma_a$ ,  $\sigma_b$  and the covariance,  $cov(a, b)$ . The correlation coefficient  $\xi$  is defined as  $\xi = cov(a, b)/\sigma_a\sigma_b$  and is shown in Fig. 2 as a function of the average of the radiative correction factor  $\langle C_R \rangle$ , weighted over  $\epsilon$ .

As the radiative corrections become larger, the correlation between the two parameters also becomes larger, reaching values near its maximum (in absolute value). Full correlation means that the two parameters are related through a constraint, i.e. it is possible to find a one-parameter description of the data.

The data shown in Fig. 2 correspond to those sets of experiments where the necessary information on the radiative corrections is available. The correlation coefficient itself can be calculated for a larger number of data and it is very large for all recent unpolarized measurements.

At low  $Q^2$  a correlation still exists, but it is smaller. For the data from Ref. [18] the radiative corrections are of the order of 15%, seldom exceed 25% and correspond to  $\epsilon < 0.8$ . This allows a safer extraction of the FFs.

Fig. 2 shows that, for each  $Q^2$ , the extraction of FFs by a two parameter fit may be biased by the  $\epsilon$  dependence induced by the radiative corrections. Whatever the precision of the individual measurements is, the slope of the reduced cross section is not sensitive to  $G_E(Q^2)$  at large  $Q^2$ . The  $Q^2$  dependence is therefore driven by  $G_M(Q^2)$ , which follows a dipole form. For each  $Q^2$  a nonzero value of the ratio  $R$  will lead to an apparent dipole dependence of  $G_E(Q^2)$ . Therefore experiments based on this method, will always give a  $Q^2$  dependence of  $G_E(Q^2)$  which is driven by  $G_M(Q^2)$ , i.e. follow approximately a dipole behavior.

### 3 Radiative corrections

It is known [16] that the process of emission of hard photons by initial and scattered electrons plays a crucial role, which results in the presence of the radiative tail in the distribution on the scattered electron energy. We give here an application of the structure function method and compare different calculations of radiative corrections. We show that they can affect the electric and magnetic part of the unpolarized cross section, and change in particular its  $\epsilon$  dependence. The main point of interest here is to show the very sharp dependence of the initial state emission on the inelastic tail of the scattered electron energy spectrum. A more extended version of this calculation and its application to polarization observables, including two photon exchange, can be found in [20].

The structure functions (SF) approach extends the traditional one [13], taking precisely into account the contributions of higher orders of perturbation theory and the role of initial state photon emission. The cross section is expressed in terms of SF of the initial electron and of the fragmentation function of the scattered electron energy fraction. Experimentally the detection of the scattered electron does not allow to separate the collinear photon emission. Therefore, one integrates in a range of the scattered electron energy. This is equivalent to set the fragmentation function to unity, due the well known properties of this formalism [16]. Initial state photon emission is more important than final state photon emission, due to the effect of decreasing  $Q^2$ . Proton emission is essentially smaller than the electron one, and can be included as a general normalization. Vacuum polarization, which has been often neglected in previous analysis, here is taken into account.

The four momentum transfer squared can be written as:  $Q^2 = 2E^2(1 - \cos\theta)/\rho$ , where  $\rho$  is the recoil factor:  $\rho = 1 + (1 - \cos\theta)(E/M)$ . In an experiment, the selection of elastic scattering requires the integration of the events in the elastic peak, and the rejection of inelastic events. We parametrize the cut on the energy of the final electron  $E'$ , selecting events with  $E' > cE/\rho$ , where  $c$  is the 'inelasticity' cut,  $c < 1$  (for the present numerical application we choose  $c = 0.97$ ).

Therefore, the differential cross section, calculated in frame of the SF method,  $\frac{d\sigma^{SF}}{d\Omega}$ , can be written as:

$$\frac{d\sigma^{SF}}{d\Omega} = \frac{\alpha^2 \cos^2(\theta/2)}{4E^2 \sin^4(\theta/2)} \int_{z_0}^1 dz D(z) \frac{\phi(z)}{[1 - \Pi(Q_z^2)]^2} \left(1 + \frac{\alpha}{\pi} K_{unp}\right). \quad (4)$$

where  $K_{unp}$  is an  $\epsilon$ -independent quantity of the order of unity, which includes all the non-leading terms, as two photon exchange and soft photon emission. More precisely the interference between the two virtual photon exchange amplitude and the Born amplitude and the relevant part of the soft photon emission i.e., the interference between the electron and proton soft photon emission, may be included in the term  $K$ . This effect is not enhanced by large logarithm (characteristic of SF) and can be included in non-leading contributions. The factor  $1 + \frac{\alpha}{\pi} K_{unp}$  can be considered as a general normalization. Here we focus on the  $\epsilon$ -dependence of the differential cross section. In order to compare the radiative corrections, we proceed as follows: we calculate the Born cross section (Eq. (1)) using dipole form factors. This result is equivalent to take the measured data and apply the 'standard' radiative corrections. The SF calculation, Eq. (4), can be expressed as a correction to the Born reduced cross section (we omit RC of higher order):

$$\sigma_{red}^{SF} = \sigma_{red}^{Born} (1 + \Delta^{SF}) \quad (5)$$

with

$$\Delta^{SF} = \frac{\alpha}{\pi} \left\{ \frac{2}{3} \left(L - \frac{5}{3}\right) - \frac{1}{2} (L - 1) \left[ 2 \ln \left( \frac{1}{1 - z_0} \right) - z_0 - \frac{z_0^2}{2} \right] + \right.$$

$$\frac{\alpha}{2\pi}\rho(1+\tau)(L-1)\int_{z_0}^1\frac{(1+z^2)dz}{1-z}\left[\frac{\phi(z)}{[1-\Pi(z)]^2}-\frac{\phi(1)}{[1-\Pi(1)]^2}\right], \quad L=\ln\frac{Q^2}{m_e^2}, \quad (6)$$

$m_e$  is the electron mass. The structure (radiation) function  $D(z)$  is

$$D(z)=\frac{\beta}{2}\left[\left(1+\frac{3}{8}\beta\right)(1-z)^{\frac{\beta}{2}-1}-\frac{1}{2}(1+z)\right]+O(\beta^2), \quad \beta=\frac{2\alpha}{\pi}\left[\ln\frac{Q^2}{m_e^2}-1\right]. \quad (7)$$

The lower limit of integration,  $z_0$ , is related to the 'inelasticity' cut,  $c$ , necessary to select the elastic data:

$$z_0=\frac{c}{\rho-c(\rho-1)}, \quad (8)$$

The transfer momentum and recoil factor of the scattered electron after the collinear photon emission are, respectively,  $Q_z$  and  $\rho_z$ :

$$Q_z^2=2E^2z^2(1-\cos\theta)/\rho_z; \quad \rho_z=1+z\frac{E}{M}(1-\cos\theta). \quad (9)$$

The kinematically corrected Born cross section for the scattered electron,  $\phi(z)$ , is:

$$\phi(z)=\frac{1}{\epsilon_z z^2 \rho_z (1+\tau_z)}\sigma_{red}(z), \quad \sigma_{red}(z)=\tau_z G_M^2(Q_z^2)+\epsilon_z G_E^2(Q_z^2). \quad (10)$$

with

$$\tau_z=\frac{Q_z^2}{4M^2}, \quad \frac{1}{\epsilon_z}=1+2(1+\tau_z)\tan^2(\theta/2). \quad (11)$$

The vacuum polarization for a virtual photon with momentum  $q$ ,  $q^2=-Q^2<0$ , is included as a factor  $1/[1-\Pi(Q^2)]$ , with  $\Pi(Q^2)=\frac{\alpha}{3\pi}\left[L-\frac{5}{3}\right]$ .

The calculation requires a specific procedure for the integration of the SF  $D(z)$ , which has a singularity at the upper limit of integration, Eq. (4).

The dependence of SF reduced cross section, Eqs. (5-11), on  $\epsilon$  is shown in Figs. 3a,b,c, for different values of  $Q^2=1, 3, 5$  GeV<sup>2</sup>, (solid lines). For comparison, the corresponding Born reduced cross section assuming also FFs parametrized in dipole form is shown as a dashed line, and the Born cross section, with FFs parametrized according to polarization measurements as a dash-dotted line.

One can see that  $SF$  corrections affect the  $\epsilon$  dependence of the cross section. Such effect is more important as  $Q^2$  increases and for large  $\epsilon$  values. The relative difference of the SF reduced cross section with respect to the Born reduced cross section (both assuming dipole FFs),  $\Delta^{SF}$ , is shown in Fig. 3d. For large values of  $\epsilon$ , the calculated reduced cross section can differ from the Born one by more than 7%, for  $c=0.97$ . As both calculations assume dipole FFs, the source of the difference has to be attributed to how radiative corrections are calculated and applied.

Let us stress that the main effect of this correction is to modify and lower the slope of the reduced cross section. This effect brings into qualitative and quantitative agreement FFs data issued from polarized and unpolarized measurements, as one can see from the comparison of the solid and dash-dotted lines in Figs. 3a,b,c.

Of course, the concrete value of the slope depends on the inelasticity cut. Taking  $0.95\leq c\leq 0.97$ , the slope given by the SF calculation is in complete agreement with the slope suggested by the polarization measurements.

## 4 Two-photon exchange

Let us consider two photon exchange, with a proton in the intermediate state of the box diagram.

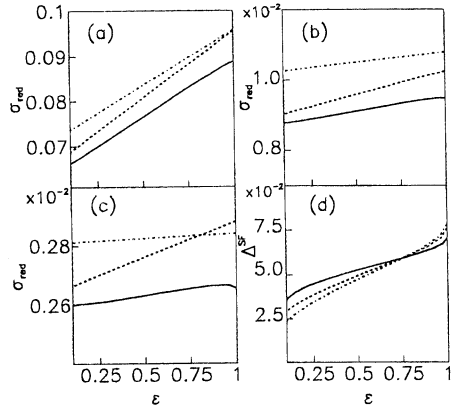


Figure 3: Reduced cross section for  $ep$  elastic scattering as a function of  $\epsilon$ , for  $c = 0.97$  at  $Q^2=1$  GeV<sup>2</sup> (a), 3 GeV<sup>2</sup> (b), and 5 GeV<sup>2</sup> (b). The SF cross section, Eq. 5, (solid line) and the Born cross section, Eq. 1, (dashed line) are shown for dipole parametrization of FFs. The relative difference between these two calculations,  $\Delta^{SF}$ , is shown in (d) for  $Q^2=1$  GeV<sup>2</sup> (solid line), 3 GeV<sup>2</sup> (dotted line), and 5 GeV<sup>2</sup> (dash-dotted line). For comparison, the calculation of the Born cross section with FFs parametrized according to [12] is shown as dash-dotted lines, in (a), (b) and (c).

In Ref. [20] the components of the recoil proton polarization (transversal  $\mathcal{P}_t$  and longitudinal  $\mathcal{P}_l$ ) were calculated in frame of the Drell-Yan approach:

$$\left(\mathcal{P}_t \frac{d\sigma}{d\Omega}\right)_{corr} = -\lambda \int_{z_1}^1 dz D(z, \beta) \frac{\alpha^2}{Q_z^2} \left(\frac{1}{\rho_z}\right)^2 \sqrt{\frac{\tau_z}{\tan^2(\theta/2)(1+\tau_z)}} G_E(Q_z^2) G_M(Q_z^2) \left(1 + \frac{\alpha}{\pi} K_t\right); \quad (12)$$

$$\left(\mathcal{P}_l \frac{d\sigma}{d\Omega}\right)_{corr} = -\lambda \int_{z_1}^1 dz D(z, \beta) \frac{\alpha^2}{2M^2} \left(\frac{1}{\rho_z}\right)^2 \sqrt{1 + \frac{1}{\tan^2(\theta/2)(1+\tau_z)}} G_M^2(Q_z^2) \left(1 + \frac{\alpha}{\pi} K_l\right). \quad (13)$$

where  $\lambda = \pm 1$  is the chirality of the initial electron;

The factors  $K_{unp}$  and  $K_{t,\ell}$  contain the contribution of the  $2\gamma$  exchange diagrams.

The loop momentum of the box-type Feynman amplitude is parametrized in such a way, that the denominators of Green function are  $(\pm\kappa + q/2)^2 + \lambda^2$  for the photon, whereas for the electron ( $e$ ) and the for the proton ( $p$ ) they have a form ( $e$ ) =  $(\pm\kappa + \Delta)^2 - m_e^2$ ,  $\Delta = \frac{1}{2}(p_1 + p'_1)$ , ( $p$ ) =  $(\kappa + \frac{1}{2}(p + p'))^2 - M^2$ , where the sign '-' for the electron corresponds to the Feynman diagram for the two photon box and the sign '+' corresponds to the crossed box diagram.

Assuming a fast decreasing of the proton form factors [19], one can neglect the dependence on the loop momentum  $\kappa$  in the denominators of photon's Green function as well as in the arguments of the form factors, which results in ultraviolet divergences of the loop momentum integrals. One obtains convergent integrals with the cut-off restriction  $|\kappa^2| < M^2\tau$ :

$$\int \frac{d^4\kappa}{i\pi^2} \frac{N_{\pm}(\Delta, Q)}{((\pm\kappa + \Delta)^2 - m_e^2)((\kappa + Q)^2 - M^2)} \theta(M^2\tau - |\kappa^2|) = I_{\pm} \cdot N_{\pm}(\Delta, Q). \quad (14)$$



where  $\Delta = \frac{1}{2}(p_1 + p'_1)$ ,  $Q = \frac{1}{2}(p + p')$ . The explicit form of  $I_{\pm}$  and  $N_{\pm}(\Delta, Q)$  can be found in [20].

Then the expressions for  $K$ -factors can be written as:

$$K_i = -2\mathcal{N} \left( Q^2/M_0^2 \right) \frac{U^i(\Delta, Q)}{Z_i}, \quad i = unp, x, z, \quad (15)$$

where  $\mathcal{N}$  is an enhancement factor:  $\mathcal{N} = F^2(Q^2/4)/F(Q^2) \simeq 2$  which is due to the fact that each photon carries half of the transferred momentum.  $Z_i$ ,  $i = unp, x, z$  are the moduli squared of the Born amplitude which are singled out in the definition of the  $K$ -factor:

$$Z_{unp} = \left( 1 - \frac{Q^2(M^2 + s)}{s^2} \right) \left[ \frac{g_e^2 + \tau g_m^2}{1 + \tau} + 2\tau g_m^2 \tan^2(\theta/2) \right], \quad (16)$$

$$Z_t = -\frac{1}{\rho} g_e g_m \sqrt{\frac{\tau}{1 + \tau}} \sin \theta, \quad Z_{\ell} = \frac{Q^2}{2E^2} g_m^2 \sqrt{\frac{\tau}{1 + \tau}} \left( \frac{E}{M} - \tau \right). \quad (17)$$

with  $g_e = 1$ ,  $g_m = \mu$  (the form factors dipole dependence is extracted as the enhancement factor  $\mathcal{N}(z)$  in (15)). In the unpolarized case the expression for  $U^{unp}(\Delta, Q)$  is:

$$\begin{aligned} U^{unp}(\Delta, Q) &= \frac{1}{s^2 M^2 \tau} \cdot \frac{1}{4} Tr \left[ (\hat{p}' + M) \Gamma_{\lambda} \hat{Q} \Gamma_{\eta} (\hat{p} + M) \bar{\Gamma}_{\mu} \right] \times \\ &\times \left\{ I_+ \cdot \frac{1}{4} Tr \left[ \hat{p}'_1 \gamma_{\lambda} \hat{\Delta} \gamma_{\eta} \hat{p}_1 \gamma_{\mu} \right] + I_- \cdot \frac{1}{4} Tr \left[ \hat{p}'_1 \gamma_{\eta} \hat{\Delta} \gamma_{\lambda} \hat{p}_1 \gamma_{\mu} \right] \right\} \end{aligned} \quad (18)$$

where  $\Gamma_{\alpha} = \gamma_{\alpha} - \frac{\mu}{4M} \gamma_{\alpha} \hat{q}$ ,  $\bar{\Gamma}_{\alpha} = \gamma_{\alpha} + \frac{\mu}{2M} \gamma_{\alpha} \hat{q}$ . The quantities  $U^{i,\ell}(\Delta, Q)$  for polarized case can be obtained from (18) by replacing  $\gamma_{\mu} \rightarrow \gamma_{\mu} \gamma_5$  in the lepton traces and  $(\hat{p}' + M) \rightarrow (\hat{p}' + M) \hat{a}_{t,\ell} \gamma_5$  in the proton traces. Here  $\hat{a}_{t,\ell}$  is the final proton polarization vector (i.e.  $(a_{t,\ell} p') = 0$ ) and corresponds to different orientations of the proton polarization. If the final proton is polarized along the  $x$ -axis, one finds:

$$(a_t p) = 0, \quad (a_t p_1) = -\frac{E^2}{2M\rho} \frac{\sin \theta}{\sqrt{\tau(1 + \tau)}}, \quad (19)$$

whereas in case of polarization along the  $z$ -axis:

$$(a_{\ell} p) = 2M \sqrt{\tau(1 + \tau)}, \quad (a_{\ell} p_1) = M \sqrt{\frac{\tau}{1 + \tau}} \left( \frac{E}{M} - 1 - 2\tau \right). \quad (20)$$

The numerical results strongly depend on the inelasticity cut, in the scattered electron energy spectrum. The results shown here correspond to  $c = 0.97$ . This value has been chosen because it corresponds to the energy resolution of modern experiments. The unpolarized cross section has been calculated assuming a dipole dependence of form factors on  $Q^2$ . In Fig. 4 the results are shown as a function of  $\epsilon$ , for  $Q^2 = 1, 3$ , and  $5 \text{ GeV}^2$ , from top to bottom. The calculation based on the structure function method is shown as a dashed line. the full calculation, including the two-photon exchange contribution is shown as the dash-dotted line. For comparison the results corresponding to the Born reduced cross section are shown as a solid line. One can see that the main effect of the present calculation is to modify and lower the slope of the reduced cross section. This effect gets larger with  $Q^2$ . Non-linearity effects are small. Including two-photon exchange modifies very little the results, in the kinematical range presented here. The relative effect on the polarization is much smaller than on the unpolarized cross section but the  $\epsilon$  dependence is different for the longitudinal and for the transversal components. Again the effect of the two photon contribution is negligible, in both cases, of the order of 1

The present results suggest that an appropriate treatment of radiative corrections constitutes the solution of the discrepancy between form factors extracted by the Rosenbluth or by the recoil polarization method.

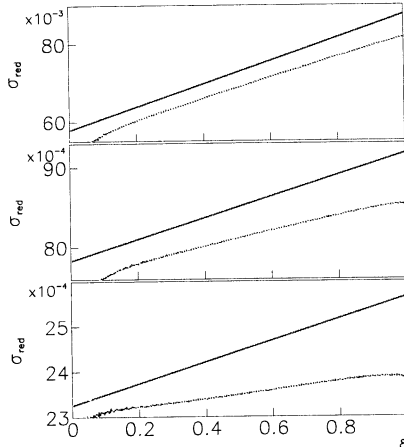


Figure 4: The  $\epsilon$  dependence of the elastic differential cross section, for  $Q^2 = 1, 3,$  and  $5$   $\text{GeV}^2$ , from top to bottom: Born cross section (solid line), Drell-Yan cross section (dashed line), full calculation (dash-dotted line).

## 5 Conclusions

We reanalyzed the Rosenbluth data with particular attention to the radiative corrections applied to the measured cross section, and we showed from the (published) data themselves that at large  $Q^2$  statistical correlations between the parameters of the Rosenbluth plot become so large that  $G_E(Q^2)$  can not be safely extracted. The method itself is biased at large momentum transfer because RC are applied as a global factor, which is the same for the electric and the magnetic contribution. Such factor contains a large  $\epsilon$ -dependence, which induces a strong correlation in the parameters of the linear  $\epsilon$  fit.

Calculations of RC in frame of the SF method, which takes into account higher order of perturbation theory, show that RC from collinear hard photon emission affect the elastic  $ep$  cross section, in particular its  $\epsilon$  dependence. Similarly to the standard RC, they depend on the electron scattering angle and on the kinematical selection for the elastic events. On the opposite, they act differently on the electric and magnetic term of the cross section, changing the slope of the reduced cross section which is related to the electric FF. When applied to the polarized cross section, their effect is small on the relevant observables. Therefore it is suggested here that such corrections, when properly applied to the experimental data, can bring into agreement the results on the proton FFs issued from unpolarized and polarized measurements. Moreover these corrections affect very little the linearity of the Rosenbluth fit, contrary to what is expected from two photon exchange [11].

We confirm the conclusion of a previous paper [3] which first suggested the polarization method for the determination of  $G_E(Q^2)$ , due to the increased sensitivity of the cross section to the magnetic term at large  $Q^2$ : *'Thus, there exist a number of polarization experiments which are more effective for determining the proton charge FF than is the measurement of the differential cross section for unpolarized particles'*.

This work was inspired by enlightening discussions with Prof. M. P. Rekaló. Thanks are due to V. Bytev for useful discussions and technical help.

## References

- [1] M. N. Rosenbluth, Phys. Rev. **79**, 615 (1950).
- [2] M. K. Jones *et al.*, Phys. Rev. Lett. **84** (2000) 1398; O. Gayou *et al.*, Phys. Rev. Lett. **88** (2002) 092301; V. Punjabi *et al.*, Phys. Rev. C **71** (2005) 055202.
- [3] A. Akhiezer and M. P. Rekalo, Dokl. Akad. Nauk USSR, **180**, 1081 (1968); Sov. J. Part. Nucl. **4**, 277 (1974).
- [4] L. Andivahis *et al.*, Phys. Rev. D **50**, 5491 (1994).
- [5] I. A. Qattan *et al.*, Phys. Rev. Lett. **94**, 142301 (2005).
- [6] M. E. Christy *et al.* [E94110 Collaboration], Phys. Rev. C **70**, 015206 (2004).
- [7] J. Arrington, Phys. Rev. C **68**, 034325 (2003).
- [8] R.G. Arnold *et al.*, Phys. Rev. Lett. **35**, 776 (1975).
- [9] P. G. Blunden, W. Melnitchouk and J. A. Tjon, Phys. Rev. Lett. **91**, 142304 (2003); P. A. M. Guichon and M. Vanderhaeghen, Phys. Rev. Lett. **91**, 142303 (2003); Y. C. Chen, A. Afanasev, S. J. Brodsky, C. E. Carlson and M. Vanderhaeghen, Phys. Rev. Lett. **93**, 122301 (2004).
- [10] E. Tomasi-Gustafsson and G. I. Gakh, Phys. Rev. C **72**, 015209 (2005).
- [11] M. P. Rekalo and E. Tomasi-Gustafsson, Eur. Phys. J. A. **22**, 331 (2004). M. P. Rekalo and E. Tomasi-Gustafsson, Nucl. Phys. A **740**, 271 (2004); M. P. Rekalo and E. Tomasi-Gustafsson, Nucl. Phys. A **742**, 322 (2004).
- [12] E. J. Brash, A. Kozlov, S. Li and G. M. Huber, Phys. Rev. C **65** (2002) 051001.
- [13] L. W. Mo and Y. S. Tsai, Rev. Mod. Phys. **41**, 205 (1969).
- [14] E. Tomasi-Gustafsson, arXiv hep-ph/0412216.
- [15] E. A. Kuraev and V. S. Fadin, Sov. J. of Nucl. Phys. **41**, 466 (1985) [Yad.Fiz. **41**, 733 (1985)].
- [16] E. A. Kuraev, N. P. Merenkov and V. S. Fadin, Sov. J. of Nucl. Phys. **47**, 1009 (1988) [Yad.Fiz. **47**, 1593 (1988)].
- [17] R. C. Walker *et al.*, Phys. Rev. D **49**, 5671 (1994).
- [18] T. Janssens, R. Hofstadter, E. B. Hughes and M. R. Yerian, Phys. Rev. **142**, 922 (1966).
- [19] J. Gunion and L. Stodolsky, Phys. Rev. Lett. **30**, 345 (1973); V. Franco, Phys. Rev. D **8**, 826 (1973); V. N. Boitsov, L.A. Kondratyuk and V.B. Kopeliovich, Sov. J. Nucl. Phys. **16**, 287 (1973); F. M. Lev, Sov. J. Nucl. Phys. **21**, 45 (1973).
- [20] Y. M. Bystritskiy, E. A. Kuraev and E. Tomasi-Gustafsson, arXiv:hep-ph/0603132.